Theory of binding energies of acceptors in semiconductors*

J. Bernholc†
Department of Theoretical Physics, University of Lund, Lund, Sweden
and IBM Thomas J. Watson Research Center, Yorktown Heights, New York 10598

Sokrates T. Pantelides
IBM Thomas J. Watson Research Center, Yorktown Heights, New York 10598

(Received 29 November 1976)

Acceptor binding energies are calculated using the full 6×6 effective-mass acceptor Hamiltonian for both shallow and deep levels. It is found that for homopolar semiconductors (Si and Ge) the method is valid for both shallow and deep acceptors, in agreement with a similar result obtained previously by Pantelides and Sah for donors in Si. Screening the impurity potential by the dielectric function $\epsilon(q)$ is again found to be very important. The point-charge model is found to be adequate for shallow single acceptors and the relatively shallow double acceptors in Ge, but completely inadequate for the deep double acceptors in Si and triple acceptors in Ge. Use of model potentials, however, which reflect the chemical nature of individual impurities, is shown to be capable of reproducing the observed values. When model potentials from the literature are used, agreement with experiment is only modest, due to a sensitivity of the calculation on the core part of the impurity potential. Similar calculations in heteropolar semiconductors (GaP, GaAs, etc.) show that good agreement is obtained only for very shallow levels. For deeper levels, effects due to differences in the anion and cation sites are dominant. It is argued that these effects lie outside the effective-mass theory.

I. INTRODUCTION

Shallow impurities have long been described by the well-known effective-mass theory (EMT).[1] In the case of levels associated with a single nondegenerate parabolic-band extremum of the form

$$E(k)=E_0+\hbar^2k^2/2m^*, \tag{1}$$

where m^* is the effective mass, the localized energy levels are determined by the Schrödinger-like equation

$$[-(\hbar^2/2m^*)\nabla^2+U(r)]F(r)=EF(r). \tag{2}$$

If the band extremum is degenerate, which is the case for acceptors in cubic semiconductors, a set of coupled differential equations is obtained.[1,2]

In Eq. (2), $U(r)$ is the perturbation potential arising from the presence of an impurity in an otherwise perfect crystal. In the early applications of the EMT, $U(r)$ was taken to be

$$U(r)=U_H(r)=-e^2/\epsilon r, \tag{3}$$

where ϵ is the dielectric constant of the host crystal. This potential corresponds to that of a point charge in a dielectric medium and, as such, could be justified only at distances outside the central cell occupied by the impurity atom. It was, nevertheless, used for all values of r in the expectation that for shallow impurities, where the localized wave function is spread over hundreds of unit cells, the contribution of the "central-cell region" would be small. This choice makes (2) and its solutions isomorphic to those of the hydrogen atom, whereby the model may appropriately be called the *hydrogenic model*.

Effective-mass theory is often identified with the hydrogenic model to the extent that the well-known breakdown of $U_H(r)$ in the central cell is described as a breakdown of the EMT itself in that region. Deviations from the hydrogenic values, often called *chemical shifts*, are then thought to lie outside the EMT. Recently, however, Pantelides and Sah[3-5] have shown that the EMT is in fact valid for a variety of potentials $U(r)$, including potentials constructed from first principles, not only for shallow levels, but for many *deep* levels as well. They introduced the distinction between *isocoric impurities*, namely those whose cores are isoelectronic with the cores of the host atoms, for which the potentials $U(r)$ may be constructed from true ionic potentials, and nonisocoric impurities, for which $U(r)$ must be constructed from appropriately chosen pseudopotentials. In the work of Refs. 3–5, it was found instructive to compare the binding energies obtained from first-principles potentials with the hydrogenic binding energy E_H obtained with the potential $U_H(r)$, and also with the binding energy E_{pc} obtained with a potential $U_{pc}(r)$ defined by screening the potential of one or more point charges by the diagonal part of the dielectric function $\epsilon(q)$. $U_{pc}(r)$, which will be referred to as the *point-charge model*, is defined by the expression

$$U_{pc}(r)=n\int d^3q\,\frac{4\pi e^2}{\epsilon(q)q^2}\,e^{i\vec{q}\cdot\vec{r}}, \tag{4}$$

where n is the number of point charges.

The problem of acceptors has recently been con-

sidered by Baldereschi and Lipari.[6,7] These authors rewrote the acceptor Hamiltonian in a manner that allowed a systematic classification of the excited states. Their study of binding energies, however, was limited to the use of the hydrogenic potential $U_H(r)$. Furthermore, binding-energy calculations were carried out only within the "spherical" approximation to the acceptor Hamiltonian.[6,7]

The purpose of this work is to provide a comprehensive study of binding energies of acceptors in tetrahedral semiconductors. In this paper, we will mainly concentrate on the hydrogenic and point-charge models, but we will also employ model potentials and indicate the prospects of a more complete theory of acceptors.

II. ACCEPTOR HAMILTONIAN

A. Kinetic energy

As noted earlier, Eq. (2) is the effective-mass equation for a simple parabolic band extremum of the form (1). The top of the valence bands in the tetrahedral semiconductors, however, is both degenerate, anisotropic and spin-orbit split. A plot of these bands for silicon along high-symmetry directions is shown in Fig. 1. At the center of the Brillouin zone, the top of the valence bands is four-fold degenerate and of Γ_8 symmetry. Away from the center of the zone, the four states split into two bands, the so-called heavy-hole band at higher energies, and the so-called light-hole band at lower energies. Finally, at an energy λ below the top, lies the spin-orbit split band, which at the center of the zone has Γ_7 symmetry. The precise form of the valence bands near the top is obtained from $\vec{k}\cdot\vec{p}$ theory[8] by diagonalizing a 6×6 matrix $D(\vec{k})$. From symmetry arguments, one can show that the matrix $D(\vec{k})$ can be expressed in terms of three parameters γ_1, γ_2, and γ_3 analogous to inverse effective masses. Accurate measurements of γ_1, γ_2, and γ_3 are available only for Si and Ge.[9,10] Parameters for other materials have been estimated by Lawaetz.[11] Given the matrix $D(\vec{k})$, the effective-mass equation, analogous to (2), becomes

$$[D(-i\nabla)+U(r)I]F(\vec{r})=EF(\vec{r}), \tag{5}$$

where I is the unit matrix of the same order as D. $F(\vec{r})$ is now a column vector.

Two approximations to the full 6×6 matrix for D have been used in the past. The first corresponds to zero spin-orbit splitting, whereby D reduces to a 3×3 matrix. This limit would be appropriate for impurities whose binding energies are much larger than the band spin-orbit splitting at Γ, most of which would be classified as deep. The second approximation corresponds to infinite spin-orbit splitting, whereby D reduces to a 4×4 matrix. This limit would be appropriate for very shallow impurities, whose binding energies are much smaller than the band spin-orbit splitting at Γ. For single acceptors, however, which are the only ones that have been studied theoretically thus far, only in a few materials is the 4×4 approximation acceptable (see below). In most cases, on the other hand, the 4×4 approximation is adequate for the study of higher excited states.

The matrix D may be written in a variety of forms,[1,2,7,8,12] which are related by unitary transformation to each other. In the case of the 4×4 approximation, a very elegant form was obtained recently by Baldereschi and Lipari.[6,7] In this form one can separate out terms with full spherical symmetry and a term with strictly cubic symmetry.[6] They later[7] included the cubic terms by first-order perturbation theory, but the contribution was nonzero only for certain excited states. In that way they obtained an elegant and systematic classification of the excited states. For quantitative calculations of binding energies, however, the method, as has been used thus far, is accurate only for cases for which the "infinite spin-orbit" approximation is adequate.[13]

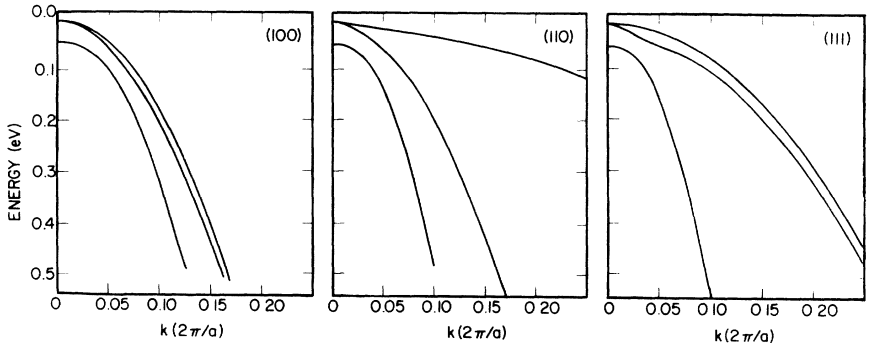

FIG. 1. Valence energy bands of Si near Γ along high symmetry directions.

B. Impurity potentials

Most previous effective-mass work on acceptors has been in terms of the hydrogenic potential $U_H(r)$. For example, Schechter[14] first solved the hydrogenic acceptor problem for Si and Ge using the "zero" and "infinite" spin-orbit splitting approximations, and treated the intermediate case by perturbation theory. Subsequently, more accurate hydrogenic solutions for Ge were obtained by Mendelson and James[15] but still using "infinite" spin-orbit splitting. Suzuki, Okazaki, and Hasegawa[12] (SOH) first solved the full 6×6 hydrogenic problem for Si and Ge, and, more recently, Mendelson and Schultz[16] obtained a still more accurate solution of this problem in Si (see Sec. III). In more recent work, Baldereschi and Lipari[6,7] used the 4×4 matrix which is less accurate for binding energies, especially for cases where the binding energy is of the same order of magnitude as the spin-orbit splitting. These various results are summarized in Table I. For completeness we included the values obtained in the present work, which were carried out as a test of the accuracy of our method, to be described in Sec. III.

In the recent work by Pantelides and Sah[3-5] it was found that the inclusion of the proper dielectric screening $\epsilon(q)$, instead of simply the dielectric constant ϵ, leads to significant changes in the binding energies of donors in Si. This result will be further confirmed here for acceptors in different materials. Pantelides and Sah introduced also a *point-charge model*, that is, a point-charge potential screened by the diagonal part of the dielectric function $\epsilon(q)$. In the case of partially ionic compounds, we will find that differences between binding energies of holes described by the point-charge model and the hydrogenic model are even more drastic, sometimes by an order of magnitude (see below).

For the zinc-blende type compounds, such as GaP, GaAs, etc., the situation is complicated further by the fact that these crystals are partially ionic whereby the lattice itself may distort to screen a foreign charge embedded in the crystal. This distortion of the lattice, often referred to as lattice polarizability, contributes to the dielectric constant and raises its value from ϵ_∞ (the electronic or high-frequency dielectric constant) to ϵ_0 (the static dielectric constant). In general, classical considerations suggest that ϵ_0 should be used for shallow levels for which binding energies are smaller than the typical phonon energies, and ϵ_∞ for deeper levels with binding energies larger than typical phonon energies. In many cases, however, single acceptor binding energies are of the same order of magnitude as typical phonon energies, but no theory is available for such intermediate cases. The calculations, therefore, at this point, can only be carried out at the two limits.

In calculating the point-charge potential $U_{pc}(r)$ from Eq. (4) one needs to know the full $\epsilon(q)$ for every crystal. These functions are not obtainable from experiment, but theoretical calculations are available for Si and Ge.[17] For our present purposes we fitted numerical results for $\epsilon(q)$ to the following analytical expression, first used by Nara[18]:

$$\frac{1}{\epsilon(q)} = \frac{1}{\epsilon(0)} + A\frac{q^2}{q^2+\alpha^2} + (1-A)\frac{q^2}{q^2+\beta^2} - \frac{1}{\epsilon(0)}\frac{q^2}{q^2+\gamma^2}. \tag{6}$$

The parameters A, α, β, γ were fitted to the numerical points.

For III-V and II-VI compounds the difficulty of including lattice polarizability in an appropriate way arises once more. Theoretical calculations are available[19] for the electronic $\epsilon(q)$ [for which $\epsilon(0)=\epsilon_\infty$], and the numerical results were once more fitted with the analytical expression (6). In order to include lattice polarizability, we scaled the calculated results according to the formula

TABLE I. Hydrogenic binding energy E_H for acceptors in Si and Ge as obtained by various authors in the past. The value of ϵ listed is that used by the respective authors.

Authors	Year	Si ϵ	Si E_H (meV)	Ge ϵ	Ge E_H (meV)
Schechter	1962	12.0	36.0	16.0	9.4
Mendelson and James	1964	...	...	16.0	9.28
Suzuki *et al.*	1964	12.0	35.7	16.0	10.0
Mendelson and Schultz	1969	12.0	37.1	...	...
Baldereschi and Lipari	1973	11.4	31.6	15.36	9.8
Present[a]	1976	12.0	37.1	16.0	11.2
Present[b]	1976	11.4	37.8	15.36	10.3

[a] Using values of γ_1, γ_2, and γ_3 from Suzuki *et al.*.
[b] Using values of γ_1, γ_2, and γ_3 from Table II.

TABLE II Band-structure parameters and dielectric functions of the semiconductors studied. $\gamma_1, \gamma_2, \gamma_3$ are the inverse masses in atomic units, λ is the spin-orbit splitting in eV, ϵ is the dielectric constant, subscript ∞ denotes ϵ_∞. A, α, β, γ are those appearing in Eq. (6). A is dimensionless, α, β, and γ are expressed in atomic units. γ_1, γ_2, γ_3, and λ are taken from Lawaetz (Ref. 11), ϵ_0 from Baldereschi and Lipari (Ref. 6), and ϵ_∞ from Van Vechten (Ref. 20).

Crystal	γ_1	γ_2	γ_3	λ	ϵ	A	α	β	γ
Si	4.28	0.375	1.45	0.044	11.4	1.104[a]	0.710[a]	0.288[a]	2.645[a]
						1.133[b]	0.798[b]	0.440[b]	2.645[b]
					11.4	1.175[c]	0.757[c]	0.312[c]	2.044[c]
Ge	13.35	4.25	5.69	0.29	15.36	1.101[a]	0.706[a]	0.295[a]	2.645[a]
						1.104[b]	0.762[b]	0.422[b]	2.645[b]
GaAs	7.65	2.41	3.28	0.34	12.56	1.105[a]	0.717[a]	0.292[a]	0.390[a]
						1.136[b]	0.794[b]	0.470[b]	2.635[b]
					10.9_∞	1.138[a]	0.762[a]	0.376[a]	2.642[a]
						1.107[b]	0.771[b]	0.432[b]	2.645[b]
GaP	4.20	0.98	1.66	0.082	10.75	1.144[b]	0.855[b]	0.448[b]	2.643[b]
					9.1_∞	1.132[b]	0.829[b]	0.442[b]	2.638[b]
GaSb	11.8	4.03	5.26	0.77	15.7	1.090[b]	0.730[b]	0.403[b]	2.636[b]
					14.4_∞	1.084[b]	0.716[b]	0.399[b]	2.646[b]
AlSb	4.15	1.01	1.75	0.75	12.0	1.132[b]	0.796[b]	0.425[b]	2.642[b]
					10.2_∞	1.113[b]	0.762[b]	0.388[b]	2.644[b]
InAs	19.67	8.37	9.29	0.38	14.6	1.102[b]	0.735[b]	0.367[b]	2.640[b]
					12.3_∞	1.089[b]	0.710[b]	0.362[b]	2.645[b]
InP	6.28	2.08	2.76	0.13	12.4	1.219[b]	0.727[b]	0.518[b]	0.519[b]
					9.6_∞	1.102[b]	0.767[b]	0.430[b]	2.646[b]
InSb	35.08	15.64	16.91	0.81	17.9	1.090[b]	0.708[b]	0.349[b]	2.642[b]
					15.7_∞	1.085[b]	0.698[b]	0.346[b]	2.641[b]
ZnS	2.54	0.75	1.09	0.068	8.1	1.198[b]	0.951[b]	0.540[b]	2.643[b]
					5.2_∞	1.159[b]	0.889[b]	0.496[b]	2.644[b]
ZnSe	3.77	1.24	1.67	0.43	9.1	1.203[a]	0.882[a]	0.476[a]	2.646[a]
						1.162[b]	0.893[b]	0.459[b]	2.642[b]
					5.9_∞	1.170[a]	0.832[a]	0.478[a]	2.634[a]
						1.139[b]	0.841[b]	0.451[b]	2.645[b]
ZnTe	3.74	1.07	1.64	0.92	10.1	1.245[b]	0.707[b]	0.508[b]	0.515[b]
					7.3_∞	1.102[b]	0.778[b]	0.457[b]	2.645[b]
CdTe	5.29	1.89	2.46	0.91	9.7	1.136[b]	0.813[b]	0.444[b]	2.645[b]
					7.2_∞	1.106[b]	0.760[b]	0.409[b]	2.635[b]

[a] Fitted to results by Walter and Cohen (Ref. 17).
[b] Fitted to results by Vinsome and Richardson (Ref. 19).
[c] Fitted to results by Nara (Ref. 18).

$$\epsilon(q) = [\,\epsilon_{\text{calc}}(q) - 1\,]\,\frac{\epsilon_{\text{expt}}(0) - 1}{\epsilon_{\text{calc}}(0) - 1} + 1 \tag{7}$$

so that $\epsilon(0) = \epsilon_0$ and fitted anew. Since $\epsilon_{\text{calc}}(0)$ was different from $\epsilon_{\text{expt}}(0)$ for both Si, Ge, and the compounds, we used (7) in order to reproduce the experimental values. All our fitting parameters for dielectric functions together with band structure parameters used here are listed in Table II. In Fig. 2 we show the three different functions $\epsilon(q)$ employed in the calculations.

III. METHOD OF CALCULATION

Equation (5) has been solved only variationally thus far. The column vectors $F(\vec{r})$ are expressed in terms of spherical harmonics and may be written as follows:

$$F(\vec{r}) = \sum_l \sum_m f_{lm}(r) G_{lm}(\theta, \phi), \tag{8}$$

where $f_{lm}(r)$ are simple radial functions to be determined variationally and $G_{lm}(\theta, \phi)$ are column

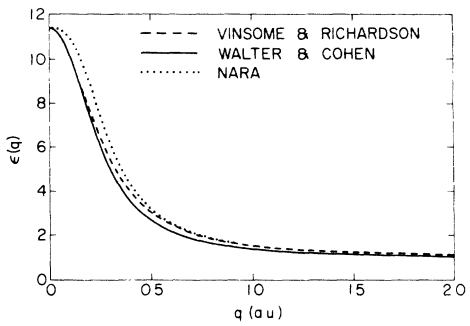

FIG. 2. $\epsilon(q)$ for Si from various references as used in the calculations. See Table II for the parameters used.

vectors determined entirely from symmetry considerations.[12] Since the effective-mass equations have inversion symmetry, only even l will contribute to the ground-state wave function. Following previous workers, we assume that the ground state has the same symmetry as the top of the valence bands, i.e., Γ_8. This has been proved experimentally by Onton *et al.*[21] We use the same representation as SOH[12] and include only s and d waves. This leaves us with one s and five d angular trial functions. The form of $f_{lm}(r)$ used by Schechter[13] and SOH is

$$f_{l=0}(r)=e^{-r/r_1}, \qquad f_{l=2}(r)=r^2e^{-r/r_2}, \tag{9}$$

where r_1 and r_2 are variational parameters. In order to enhance the flexibility of the trial form of $F(\vec{r})$ we expanded $f_{lm}(r)$ as

$$f_{lm}(r)=\sum_i \sum_n C_{lmni} r^n e^{-r/r_i}. \tag{10}$$

For $l=0$, n was taken to be 0 and 1, and for $l=2$, n was taken to be 1 and 2. The r_i were taken to be the same for each l and n. Thus, for N different r_i, the number of independent basis functions (and hence the size of the secular matrix) is $12N$. In this scheme, by solving the generalized eigenvalue problem $HX=ESX$ only once, the binding energy is determined as the highest eigenvalue.

The r_i were chosen to cover a broad range. The starting point was five r_i, namely the inverses of 0.01, 0.05, 0.1, 0.2, and 0.4 a.u. These values correspond to orbits of 100, 20, 10, 5, and 2.5 a.u. The set was then extended to include additional intermediate values, but the calculated binding energy changed only by about 1% in all materials. In any case, all calculations were finally performed with an expanded set, namely the inverses of 0.01, 0.02, 0.03, 0.04, 0.05, 0.1, 0.2, and 0.4 a.u., which correspond to orbits of 100, 50, 33.3, 25, 20, 10, 5, and 2.5 a.u. The size of the secular matrix was 96×96. It was concluded that the binding energies quoted are converged to at least 0.2% (within our angular expansion). As an additional test for the accuracy of our method of calculation we used the same Hamiltonian parameters and hydrogenic potential for Si and Ge as used by SOH and Mendelson and James[14] ($\epsilon=12$ and 16 for Si and Ge, respectively). For Si we obtained 37.1 meV, compared with SOH's 35.7 meV and Mendelson and James's 37.1 meV, indicating that our method is better than that of SOH and as good as that of Mendelson and James. Similarly, for Ge we obtained 11.2 meV as compared with SOH's 10.0 meV.

IV. SINGLE ACCEPTORS

A. Hydrogenic model

Using the full 6×6 Hamiltonian, as described earlier, we carried out calculations for single acceptors employing the hydrogenic potential. The dielectric constants were the same as those used by Baldereschi and Lipari[6,7] (BL). In Table III we list the results of the present calculations and compare them with those of BL. In the same table we also listed the results of a 4×4 Hamiltonian and our basis. Differences between these results and

TABLE III. Hydrogenic binding energies E_H in meV as calculated in this paper by full spin-dependent Hamiltonian, in infinite spin-orbit approximation and as calculated by BL in the same approximation using the spherical model. For our 6×6 calculations we also list the percent of s-like envelope (% s), the percent of d-like envelope (% d), the expectation value of r (average radius) for the s envelope ($\langle r_s\rangle$), the average d-envelope radius ($\langle r_d\rangle$), and the total average radius ($\langle r\rangle$). r is in atomic units.

		Present 6×6						Present 4×4	BL
Material	ϵ_0	% s	% d	$\langle r_s\rangle$	$\langle r_d\rangle$	$\langle r\rangle$	E_H	E_H	E_H
Si	11.4	87	13	43.6	83.2	48.6	37.8	33.3	31.56
Ge	15.36	73	27	110	229	142	10.3	10.0	9.73
GaAs	12.56	74	26	49.9	106	64.4	27.5	26.3	25.67
GaP	10.75	83	17	29.7	61.5	35.3	56.3	49.5	47.40
GaSb	15.7	70	30	82.4	176	111	13.1	12.9	12.55
AlSb	12.0	77	23	31.7	64.6	39.2	46.7	44.9	42.45
InAs	14.6	62	38	60.7	145	92.8	17.3	16.8	16.31
InP	12.4	75	25	33.8	75.1	44.1	40.3	36.3	35.20
InSb	17.9	58	42	93.4	231	151	8.81	8.73	8.55
ZnS	8.1	79	21	9.69	21.5	12.2	224	183	175.6
ZnSe	9.1	75	25	14.7	32.6	19.2	126	114	110.2
ZnTe	10.1	75	25	19.8	41.9	25.4	86.5	81.8	77.84
CdTe	9.7	67	31	17.3	39.4	24.2	96.6	90.7	87.26

TABLE IV. Hydrogenic binding energies E_H in meV for compound semiconductors using ϵ_∞ instead of ϵ_0. The quantities listed are as in Table III.

Material	ϵ_∞	%s	%d	$\langle r_s \rangle$	$\langle r_d \rangle$	$\langle r \rangle$	E_H
GaAs	10.9	75	25	42.8	91.3	55.1	36.9
GaP	9.1	83	17	24.8	51.6	29.5	79.7
GaSb	14.4	70	30	75.4	161.3	101.5	15.6
AlSb	10.2	78	22	26.6	54.6	32.8	65.4
InAs	12.3	63	37	50.6	122	77.2	24.6
InP	9.6	76	24	25.5	57.0	33.0	69.2
InSb	15.7	58	42	81.9	202	132	11.5
ZnS	5.2	79	21	6.16	13.8	7.81	552
ZnSe	5.9	77	23	9.10	20.5	11.8	315
ZnTe	7.3	76	24	13.8	29.7	17.7	170
CdTe	7.2	70	30	12.5	28.8	17.3	181

those of BL are to be attributed strictly to the neglect of the cubic terms by BL. The differences between the present 6×6 results and those of BL are to be attributed to the neglect of both cubic terms and the split-off band by BL. We note that the differences are largest for materials with small spin-orbit splitting like Si, GaAs, and ZnS. For Si, neglecting the cubic terms within the "infinite spin-orbit coupling" approximation is an error of about 5%. Neglecting both the cubic terms and the split-off band is an error of about 20%. As we shall see later, for other potentials the error is even larger. Finally, in Table IV we list the results of calculations using the full 6×6 EMT Hamiltonian and ϵ_∞ for the compound semiconductors instead of ϵ_0.

B. Point-charge model

We have carried out calculations using the point-charge potential as defined by (4) using the func-

TABLE V. Point-charge binding energies E_{pc} in meV for single acceptors. The references identify the $\epsilon(q)$ used (the analytical form parameters are listed in Table II). The labeling by ϵ_∞ or ϵ_0 indicates whether $\epsilon(0)=\epsilon_\infty$ or ϵ_0 as discussed in Sec. II B. For comparison we also list E_{pc} obtained within "infinite" and "zero" spin-orbit splitting, respectively. We also give the experimental values (Ref. 5). All other quantities are as in Table III.

	$\epsilon(q)$	Full 6×6						4×4	3×3	Experiment	
Material	Reference	%s	%d	$\langle r_s \rangle$	$\langle r_d \rangle$	$\langle r \rangle$	E_{pc}	E_{pc}	E_{pc}	E_B	Impurity
Si	ϵ_0[a]	86	14	30.2	58.4	34.2	54.4	39.9	57.1	68.9	Al
	ϵ_0[b]	86	14	32.7	63.2	37.0	50.2	38.8	52.7		
	ϵ_0[c]	87	13	36.5	70.1	41.0	44.8	36.4	47.2		
Ge	ϵ_0[a]	73	27	105	220	136	10.7	10.3	13.3	10.8	Ga
	ϵ_0[b]	73	27	106	220	136	10.7	10.3	13.3		
GaAs	ϵ_0[a]	74	26	41.7	90.3	54.3	32.6	28.9	40.4	31.0	Zn
	ϵ_0[b]	74	26	37.5	82.1	49.0	36.3	30.8	45.6		
	ϵ_∞[a]	75	25	31.1	68.9	40.6	50.2	41.3	62.0		
	ϵ_∞[b]	75	25	29.1	65.0	38.1	53.7	42.8	66.4		
GaP	ϵ_0[b]	81	19	15.7	33.7	19.1	110	67.7	116	64.0	Zn
	ϵ_∞[b]	81	19	11.4	24.8	14.0	185	105	192		
GaSb	ϵ_0[b]	69	31	73.0	158	99.1	14.7	14.0	19.4	13–15	Si
	ϵ_∞[b]	69	31	65.2	141	88.6	17.9	16.9	23.8		
AlSb	ϵ_0[b]	78	22	8.82	19.6	11.2	198	86.5	248		?
	ϵ_∞[b]	78	22	6.49	14.3	8.19	353	147	411		
InAs	ϵ_0[b]	63	37	48.8	121	75.7	21.3	18.9	28.9		
	ϵ_∞[b]	64	36	36.4	92.2	56.7	33.8	27.9	45.5		
InP	ϵ_0[b]	76	24	13.2	31.4	17.6	112	55.3	124	56.3	Cd
	ϵ_∞[b]	76	24	8.26	19.9	11.1	256	112	269		
InSb	ϵ_0[b]	58	42	86.1	215	140	9.54	9.3	13.1	~10	Cd
	ϵ_∞[b]	58	42	73.9	185	120	12.7	12.2	17.5		
ZnS	ϵ_0[b]	77	23	3.88	4.56	4.04	2386	1175	2393		
	ϵ_∞[b]	77	23	3.68	3.91	3.73	4076	2472	3973		
ZnSe	ϵ_0[a]	76	24	3.82	6.83	4.55	1205	497	1233	114	Li
	ϵ_0[b]	76	24	3.78	6.78	4.52	1229	492	1278		
	ϵ_∞[a]	76	24	3.19	5.22	3.68	2438	1299	2450		
	ϵ_∞[b]	76	24	3.19	5.22	3.69	2431	1257	2443		
ZnTe	ϵ_0[b]	77	23	3.81	7.66	4.71	986	397	1078		
	ϵ_∞[b]	77	23	3.28	6.17	3.95	1708	813	1786		
CdTe	ϵ_0[b]	74	26	3.60	7.11	4.53	1231	472	1335		
	ϵ_∞[b]	74	26	3.16	5.82	3.85	2065	964	2145		

tions $\epsilon(q)$ of Table II. The results are listed in Table V. Note that the three available $\epsilon(q)$ for Si give binding energies which differ by more than 10%. Since it is not possible to assess the accuracy of the three available $\epsilon(q)$, this variation may be viewed as a limit of how accurately the binding energy of the point-charge model may be calculated at this point. The results also show that a very careful treatment of the dielectric response is necessary for any calculation of binding energies. A comparison with Table III shows that the q-dependent dielectric screening is very important indeed. The differences between E_{pc} and E_H for very shallow levels like those of Ge, GaAs, GaSb, and InSb are only (4–23)%, but in Si, GaP, AlSb, and InP the increase in binding energy is 47, 95, 326, and 178%, respectively. The most dramatic effect is observed in II-VI compounds where the binding energy increases by an order of magnitude!

The values obtained using ϵ_∞ in the case of compounds show similar trends. Since ϵ_∞ is less than ϵ_0, the impurity radius becomes smaller. Therefore, the effect of $\epsilon(q)$ is even greater.

In Table IV we list also values obtained with "infinite" and "zero" spin-orbit splitting. The "infinite-splitting" approximation is expected to work well when $E_B \ll \lambda$. Direct comparison shows that this approximation is justified for Ge, GaSb, InSb (error less than 4%) and maybe for GaAs and InAs (error $\approx$ 14%). The "zero splitting" approximation should be valid when $E_B \gg \lambda$. Direct comparison shows that this approximation works well in Si, GaP, InP, ZnS, ZnSe, ZnTe, and CdTe (error < 10%). For Si, GaP, and InP these results are somewhat surprising since the binding energies of the point-charge model are comparable to the spin-orbit splitting. One should therefore be very careful in using this approximation for these materials, especially since the above results were derived using the point-charge model.

V. DOUBLE AND TRIPLE ACCEPTORS

The work of Pantelides and Sah[3,4] has shown that double donors may be treated by the EMT as long as the impurity potentials are appropriately constructed. It is thus natural to compare with a two-charge hydrogenic potential and the two-point-charge potential screened with $\epsilon(q)$. In some materials, such as Ge, where the effective masses are very small, the EMT may be adequate even for triple acceptors where one would compare with three-charge models. We have carried out these model calculations for double and triple acceptors, and the results are listed in Tables VI–VIII. Comparing the results for double acceptors we see that the binding energies derived from the hydrogenic model and point-charge model differ by an order of magnitude in all cases except Ge. We also notice that for the point-charge model the zero spin-orbit splitting approximation works well in Si, GaAs, GaP, AlSb, InAs, and InP, whereas the "infinite" spin-orbit approximation does not work in any case. We have not listed the II-VI compounds since the binding energies in the point-charge model become more than 5 eV. For the same reason we only list Ge in the triple acceptor case. The three-point-charges model gives a very deep level and consequently may be well described

TABLE VI. Hydrogenic calculations for double acceptors. All quantities are defined in the text and previous tables.

Material	ϵ	%s	%d	Full 6×6 $\langle r_s \rangle$	Full 6×6 $\langle r_d \rangle$	$\langle r \rangle$	E_{2H}	4×4 E_{2H}	3×3 E_{2H}
Si	11.4	86	14	21.0	41.2	23.9	157	133	160
Ge	15.36	75	25	52.3	112	67.1	42.9	40.2	50.5
GaAs	12.56	77	23	23.3	50.9	29.7	117	105	133
	10.9_∞	78	22	20.0	43.7	25.3	158	140	176
GaP	10.75	82	18	14.3	30.1	17.1	236	198	243
	9.1_∞	82	18	12.0	25.5	14.4	332	277	339
GaSb	15.7	71	29	39.8	86.7	53.5	53.8	51.5	66
	14.4_∞	71	29	36.2	79.3	48.7	64.3	61.3	78.4
AlSb	12.0	79	21	14.8	31.0	18.2	198	180	226
	10.2_∞	80	20	12.4	26.0	15.1	279	249	313
InAs	14.6	66	34	28.7	70.7	43.1	73.3	67.1	88.4
	12.3_∞	67	33	23.7	59.0	35.3	105	95	125
InP	12.4	77	23	15.9	35.8	20.4	174	145	185
	9.6_∞	77	23	12.1	27.6	15.6	296	242	308
InSb	17.9	59	41	45.8	114	73.7	36.1	34.9	46.6
	15.7_∞	60	40	39.8	100	64.0	47.3	45.5	60.5

TABLE VII. Point-charge calculations for double acceptors. All quantities are defined in the text and previous tables.

Material	ϵ	% s	% d	Full 6×6 $\langle r_s \rangle$	Full 6×6 $\langle r_d \rangle$	Full 6×6 $\langle r \rangle$	E_{2pc}	4×4 E_{2pc}	3×3 E_{2pc}
Si	ϵ_0 [a]	83	17	3.65	6.61	4.15	2351	1018	2354
	ϵ_0 [b]	83	17	4.23	7.86	4.84	1638	662	1641
	ϵ_0 [c]	83	17	4.45	8.30	5.11	1409	569	1398
Ge	ϵ_0 [a]	76	24	29.0	66.0	37.9	76.9	51.0	92.9
	ϵ_0 [b]	76	24	30.8	69.8	40.2	72.4	50.8	87.4
GaAs	ϵ_0 [a]	76	24	4.25	8.98	5.37	1389	430	1427
	ϵ_0 [b]	76	24	4.00	8.24	5.00	1713	581	1751
	ϵ_∞ [a]	77	23	3.68	7.66	4.62	2057	835	2096
	ϵ_∞ [b]	77	23	3.57	7.43	4.48	2229	941	2268
GaP	ϵ_0 [b]	80	20	3.70	4.73	3.91	4162	2036	4170
	ϵ_∞ [b]	80	20	3.36	4.47	3.58	5027	2920	5036
GaSb	ϵ_0 [b]	75	25	6.64	16.2	9.06	515	141	592
	ϵ_∞ [b]	75	25	5.87	14.3	7.99	670	209	750
AlSb	ϵ_0 [b]	79	21	4.19	3.85	4.11	6763	3707	6841
	ϵ_∞ [b]	79	21	3.77	3.80	3.78	7668	4875	7746
InAs	ϵ_0 [b]	71	29	4.02	10.4	5.89	1303	324	1356
	ϵ_∞ [b]	71	29	3.55	9.12	5.16	1821	611	1874
InP	ϵ_0 [b]	76	24	3.66	4.74	3.92	4672	2153	4688
	ϵ_∞ [b]	76	24	3.40	4.36	3.63	6173	3509	6189
InSb	ϵ_0 [b]	68	32	8.62	25.6	14.1	263	68.5	344
	ϵ_∞ [b]	68	32	7.18	21.0	11.6	387	109	475

in terms of the "zero" spin-orbit splitting approximation. For further discussion see Sec. VI.

VI. SCRUTINY OF THE HYDROGENIC AND POINT-CHARGE MODELS: COMPARISON WITH EXPERIMENT

In Secs. I–V we presented an assortment of calculations of acceptor binding energies using the effective-mass equations, the hydrogenic potential, and the point-charge potential. In this section we turn to examine the question of what all these calculations mean and how relevant they are to real situations. The discussion is distinctly different for homopolar and heteropolar semiconductors, so we treat the two classes separately.

A. Homopolar semiconductors

The homopolar semiconductors (Si, Ge) are simpler because there is no distinction between the static and the high-frequency dielectric constant. Let us start with Ge. For the single acceptors we use two theoretical binding energies, the hydrogenic $E_H = 10.3$ meV and the point-charge $E_{pc} = 10.7$ meV. This latter value compares very well with the experimental value of Ge:Ga (10.97 meV)[22] which is the isocoric acceptor. On the other hand, the two calculations show that the precise nature of the impurity potential in the central cell can easily produce changes in the binding energy of order 0.5 meV. This may be compared with the observed binding energies for B, Al, Ga, and In

TABLE VIII. Triple-acceptor calculations for Ge. All quantities are defined in the text and previous tables.

Material	ϵ	% s	% d	Full 6×6 $\langle r_s \rangle$	Full 6×6 $\langle r_d \rangle$	Full 6×6 $\langle r \rangle$	E	4×4 E	3×3 E
				Hydrogenic model					
Ge	15.36	77	23	33.4	72.9	42.5	100.4	90	113.6
				Point-charge model					
Ge	$\epsilon(q)$ [a]	76	24	4.90	11.3	6.42	1442	373	1475
	$\epsilon(q)$ [b]	76	24	5.49	12.7	7.21	1152	310	1185

in Ge, i.e., 10.47, 10.80, 10.97, and 11.61 meV,[22] respectively, which shows that individual binding energies might be reproducible if individual potentials were to be calculated for each impurity. The smallness of these chemical shifts, however, would call for an extremely accurate calculation of these potentials. In contrast, potentials such as those used by Pantelides and Sah cannot be expected to yield binding energies which are accurate by better than 1 meV. It appears then, that we can conclude that the effective-mass theory is entirely adequate for the shallow acceptors in Ge.

Turning to the double acceptors, we note that $E_{2H}=42.9$ meV and $E_{2pc}=72.4$ or 76.9 meV depending on whose $\epsilon(q)$ we use. When we compare with the experimental binding energy of the isocoric Ge:Zn (95 meV),[23] we see that the point-charge model again does very well, whereas the hydrogenic model does very poorly. Again, one would expect that individual binding energies should be obtainable within the EMT, when appropriate impurity potentials are constructed (see Sec. VIII). [An interesting observation is in order here: Note that E_{2pc} is found to be 92.9 meV (Table VII) when a 3×3 Hamiltonian matrix is employed, namely when spin-orbit interaction is excluded. This is in excellent agreement with the observed value of 95 meV for Ge:Zn. This agreement is, however, misleading because the full 6×6 matrix is an improved Hamiltonian, which, nevertheless, does not do as well.]

Finally, we turn to the calculations for triple acceptors. E_{3H} is found to be 100.4 meV and E_{3pc} soars to 1152 and 1442 meV for the two $\epsilon(q)$. Since the experimental binding energy for the isocoric Ge:Cu is 530 meV,[23] it is clear that the point-charge model overestimates it substantially. The use of realistic impurity potentials is thus imperative. (See Sec. VII.)

We turn now to Si. The hydrogenic binding energy E_H is 37.8 meV, whereas E_{pc} ranges from 44.8 to 54.4 meV. The observed value for the isocoric Si:Al is 68.9 meV,[21] i.e., about 30% larger. This is not entirely satisfactory and does not lead to a definite conclusion. One might argue that these results show how well the point-charge model can do. However, one might also argue that the valence bands of Si are strongly anisotropic,[6,7] hence the inclusion of $l=4$ terms in the trial function might increase the binding energy substantially. In any case, the new point-charge binding energy of about 50 meV is substantially larger than the best previous value of 37.1 meV.[16] If one were to measure "chemical shifts" from the new value, the chemical shift for Si:B ($E_B=44$ meV) would be negative.

For double acceptors in Si, we find $E_{2H}=157$ meV and E_{2pc} ranging from 1409 to 2351 meV. Since the observed value for Si:Zn is 617 meV,[24] it is clear that the model is inadequate. In fact, the situation is similar to that of triple acceptors in Ge. The use of realistic potentials is thus again imperative in order to check the viability of the EMT for such deep impurities. Needless to say, the study of triple acceptors in Si by the point-charge model is out of the question.

B. Heteropolar semiconductors

The discussion of the results for the heteropolar semiconductors is a far more complicated task. First we single out two semiconductors, namely GaSb and InSb. For GaSb we obtained $E_H(\epsilon_0)=13.1$ meV, $E_H(\epsilon_\infty)=15.6$, $E_{pc}(\epsilon_0)=14.7$, and $E_{pc}(\epsilon_\infty)=17.9$ meV. The differences are not that great but in view of the fact that optical phonon frequencies in this material are ~28 meV, the approximation $E_{pc}(\epsilon_0)$ should be the most appropriate. Indeed, it compares very well with the observed values of 13–15 meV.[25] Similar results apply for InSb for which $E_{pc}(\epsilon_0)=9.54$ meV and the experimental value is ~10 meV.[26] These two materials behave like Ge, whereby the values E_{2pc} (Table VII) may also be viewed as substantially correct for double acceptors. For these deep levels, however, the values $E_{2pc}(\epsilon_\infty)$ would be more appropriate. No experimental numbers are available for comparison.

For the other materials listed in the tables, the situation is more complicated. First, the single acceptor binding energies are of the same order of magnitude as the optical-phonon frequencies. This fact makes both limits (ϵ_0 or ϵ_∞) inappropriate approximations. Besides, other considerations enter which limit the usefulness of effective-mass calculations. The situation can be best illustrated by an example. Let us take single acceptors in GaP. BL used ϵ_0 and calculated a hydrogenic binding energy of 47.4 meV, which they compared with the observed value for GaP:Zn_{Ga} (this notation stands for Zn at a Ga site in GaP), i.e., 64 meV.[27] The agreement was encouraging in view of the spherical approximation and the 4×4 Hamiltonian matrix used. Our present calculations show that $E_H(\epsilon_0)=56.3$ meV which is a definite improvement. Note, however, what happens when we turn to the point-charge model. If we use a 4×4 Hamiltonian matrix, we get $E_{pc}(\epsilon_0)=67.7$ meV, which is in excellent agreement with the experimental value of 64 meV. If, however, we use the full 6×6 Hamiltonian matrix, we get $E_{pc}(\epsilon_0)=110$ meV which is in strong disagreement with the experimental value. Even worse, if we use $\epsilon_\infty(q)$ instead of $\epsilon_0(q)$, we get an even larger

binding energy, $E_{pc}(\epsilon_\infty)=185$ meV. What are we to conclude from all this? First we should note that comparison with the experimental binding energy of GaP:Zn_{Ga} is not an adequate test. GaP:Si_P is also an isocoric acceptor, and its observed binding energy is 204 meV.[28] Now, it is clear that $E_{pc}(\epsilon_\infty)$, i.e., 185 meV, agrees very well with 204 meV, and it would appear that we have something for everything. In fact, a more fundamental scrutiny is in order. It turns out that the most important consideration, which we left out so far, is the nature of the two different substitutional sites, the anion and the cation, an effect discussed recently by Phillips[29] and by Pantelides.[5] The experimental values, 64 meV for GaP:Zn_{Ga} (and similar numbers for other single acceptors at the Ga site) and 204 meV for GaP:Si_P (and similar numbers for other single acceptors at the P site) suggest immediately that no single point-charge calculation can agree well with both. Clearly the *site* must be built into the calculation; it would enter in two places: First, in screening; this is expected from the fact that the valence-electron cloud is concentrated more on the anion than on the cation. For holes, therefore, screening would be more effective at the cation site, whereby one would expect smaller binding energies for cation-site acceptors, as is observed. In principle, this site-dependent screening can be included by using the full dielectric function $\epsilon(\vec{q},\vec{q}+\vec{G})$, where $\vec{G}$ are reciprocal-lattice vectors. Reciprocal-lattice vectors are, however, outside the realm of the EMT. The second place the site-dependence would enter is in the evaluation of the impurity-potential matrix element $\langle\psi|U|\psi\rangle$. Here ψ is the total impurity wave function. In the EMT, ψ is expanded in terms of the Bloch functions ψ_{nk}, which, in turn, are expanded in terms of the plane waves $e^{i(\vec{k}+\vec{G})\cdot\vec{R}}$. In the end, all the nonzero G's are dropped, which amounts to essentially a plane-wave approximation for ψ_{nk}. When this approximation is made, any site-dependence of the ψ_{nk} is dropped. However, it is well known that the Bloch functions near the top of the valence bands have amplitude mainly on the anions. This means that if nonzero G's were retained in the expression of the ψ_{nk}, the matrix element $\langle\psi|U|\psi\rangle$ would be larger when U is centered at an anion site than when it is centered at a cation site. Once more, therefore, the site dependence would result in larger binding energies for anion-site acceptors. As before, however, this site dependence can be built in by including nonzero G's, which are outside the realm of the EMT. We are therefore led to conclude that a proper description of impurities is heteropolar semiconductors must go beyond the EMT. This conclusion is further supported by the numbers we calculated thus far. Recall that we found $E_{pc}(\epsilon_0)=110$ meV and $E_{pc}(\epsilon_\infty)=185$ meV. A more correct theory which would use an $\epsilon(q)$ intermediate between $\epsilon_0(q)$ and $\epsilon_\infty(q)$ should give a well-defined E_{pc} of order 150 meV. Building in the site dependence would then bring that number down to less than 100 meV for cation acceptors and up to over 200 meV for anion acceptors, in agreement with experiment. Similar considerations apply for the other heteropolar semiconductors. Notice that for II-VI compounds the site dependence is even more pronounced. For example, in CdS, P, at a S site has $E_B\sim 1000$ meV and Na at a Cd site has $E_B\sim 170$ meV.[30]

VII. USE OF MODEL POTENTIALS

As discussed in Sec. VI, effective-mass calculations are not very promising for heteropolar semiconductors. We therefore concentrate on Si and Ge where the use of the point-charge model was encouraging. The next step is to construct impurity potentials which reflect the chemical nature of individual impurities. This was first done successfully by Pantelides and Sah[3-5] who constructed first-principles pseudopotentials for donors in Si, and showed that these could be used with effective-mass equations for relatively accurate calculations of binding energies. Agreement with experiment for individual donors was very good for both shallow and *deep* levels, and overall trends were reproduced. It was also shown that in the case of isocoric impurities, the impurity pseudopotential reduces to the "true" impurity potential, i.e, the difference between the true potentials of the impurity and host ions. Subsequently, Pantelides[31] employed Abarenkov-Heine-type model potentials from the tables of Appapillai and Heine.[32] Each ion is then described by a potential of the form

$$V(r)=\begin{cases}A, & r<r_c,\\ -n/r, & r>r_c,\end{cases} \tag{11}$$

where A is an energy (depth of a square well) and r_c is a radius. The calculated binding energies were, in general, in good agreement with the experimental values.

For acceptors, we have thus far carried out a limited study the results of which are interesting. We used the model potentials of Appapillai and Heine, but the experimental trends were not correctly reproduced (Table IX). Agreement with experiment for individual cases was very good for single acceptors in Ge but only modest in all other cases. Note, however, that even though the two-point-charges model discussed in Sec. V is entirely inadequate in Si (>1.5 eV compared with 620

TABLE IX. Binding energies in meV of single and double acceptors in Si and Ge using Appapillai-Heine model potentials and corresponding experimental values.

Impurity	Si Theor.	Si Expt.	Ge Theor.	Ge Expt.
B	43.1	44.4[a]	10.5	10.4[b]
Al	48.7	68.9[a]	10.7	10.0[b]
Ga	46.2	72.7[a]	10.6	10.8[b]
In	50.0	156.2[a]	10.7	11.2[b]
Be	486	420[c]	55.5	60[c]
Zn	428	620[d]	54.3	95[c]
Cd	488	710[c]	55.6	160[c]
Hg	403	850[c]	53.7	230[c]
Cu[e]			246.0	530[c]

[a]Reference 21.
[b]Reference 22.
[c]Reference 23.
[d]Reference 24.
[e]Model potential from J. Kollar and G. Solt, J. Phys. Chem. Solids 35, 1121 (1974).

meV for Si:Zn), the model-potential calculation gives 428 meV which is only ~30% smaller than the experimental value.

For illustration purposes, we carried out calculations using an *impurity* potential of the form (11) (this would be the case if both host and impurity ions had the same r_c) with $r_c = 2.0$ a.u. and a variable depth A. The resulting binding energy is plotted versus A in Figs. 3 and 4 for single and double acceptors in Si and in Fig. 5 for acceptors in Ge. For single acceptors the binding energy depends only weakly on the potential up to $A \sim -2.2$ Ry. For larger negative values of A the binding energy increases more and more rapidly. These

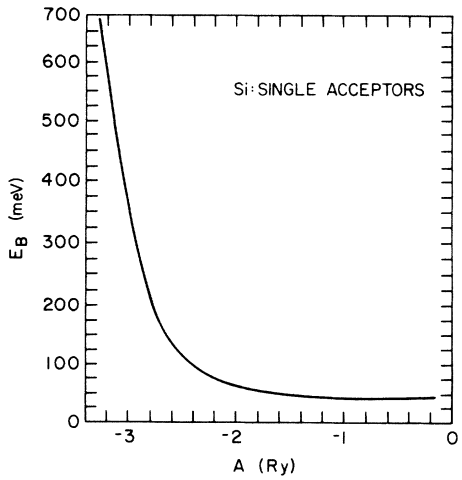

FIG. 3. Binding energy of the single acceptors in Si as a function of the depth of the potential well.

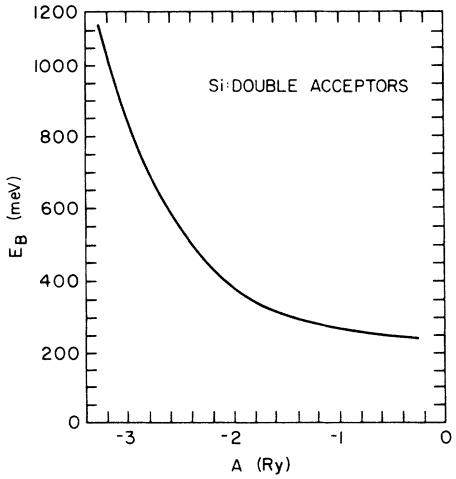

FIG. 4. Binding energy of double acceptors in Si as a function of the depth of the potential well.

results may be understood in terms of the localization of the impurity wave function as measured by the average radius (Figs. 6–8). The former situation corresponds to a hole well outside the central cell and therefore insensitive to the changes of the potential inside this region. As the strength of the potential increases, however, the hole becomes more and more localized, and small changes in the impurity potential have large effects

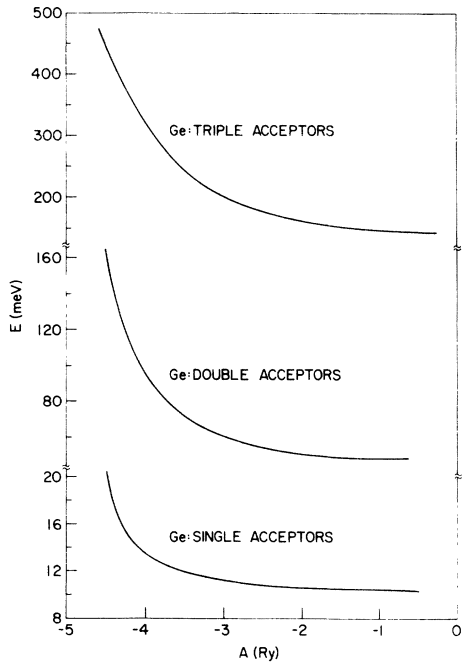

FIG. 5. Binding energy of acceptors in Ge as a function of the depth of the potential well.

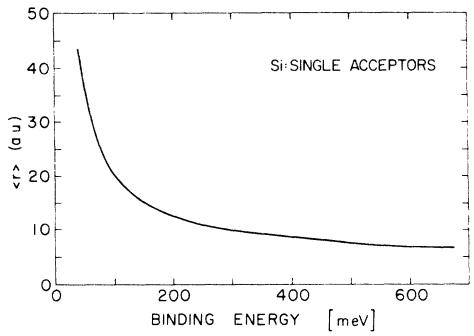

FIG. 6. Impurity radius as a function of binding energy for single acceptors in Si using a model potential as defined in text.

on the binding energy. An additional enhancement is provided by the smallness of $\epsilon(q)$ in this region. This fact makes a calculation of the impurity state with the binding energy in this range a very difficult task. For double acceptors the situation is quite similar. Since the hole is rather well localized also for small $|A|$ values, the dependence of the binding energy on the potential is greater.

Another source of inaccuracy is the dielectric functions $\epsilon(q)$ and band-structure parameters γ_1, γ_2, and γ_3. As pointed out before, the former results in errors of the order of 10% in the case of single acceptors. The double acceptors are more localized; consequently these discrepancies are even larger. The three dielectric functions used here for Si are plotted in Fig. 2. The differences among them are almost of the same order of magnitude as the differences between $\epsilon(q)$ in different directions. The $\epsilon(|q|)$ is usually obtained as an average over a very few directions. As for the γ's, they are known accurately only for Si and Ge. The values used for the compounds were those estimated by Lawaetz.

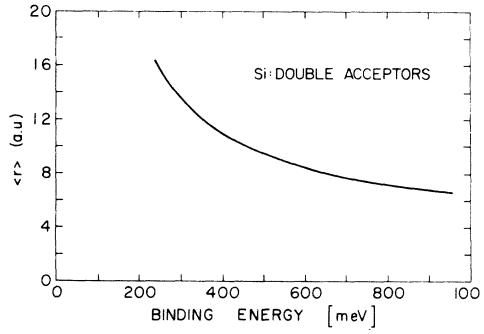

FIG. 7. Impurity radius as a function of binding energy for double acceptors in Si using a model potential as defined in text.

For heteropolar semiconductors, on the other hand, the value of the EMT appears to be limited by its inability to include effects that distinguish the cation and anion site. Our calculations show that good agreement with experiment is obtained for very shallow levels but that work beyond the EMT would be necessary to properly describe deep levels.

VIII. CONCLUSIONS

We have shown that EMT provides an adequate description of both shallow and deep acceptor states in the homopolar semiconductors, Si and Ge. For shallow levels the isocoric impurities may be described by the "point-charge model." For deeper levels it is necessary to construct the impurity potential from atomic pseudopotentials. For both shallow and deep impurity states it is essential to include the q dependence of the dielectric screening into the calculation. The determina-

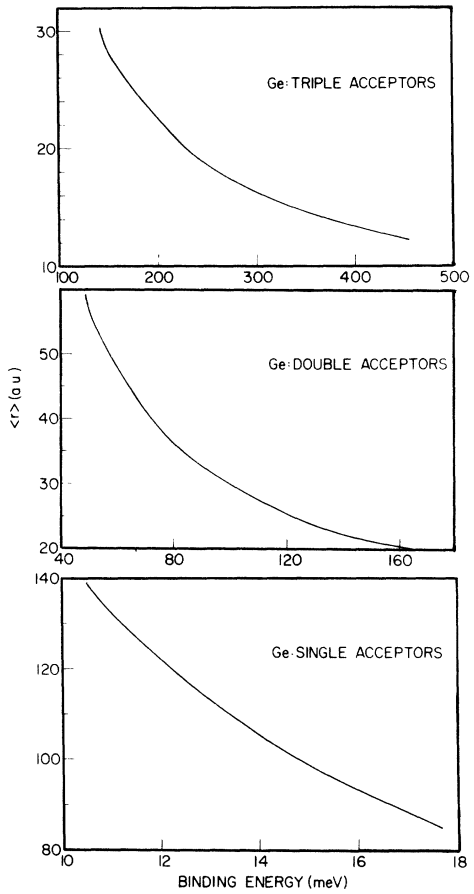

FIG. 8. Impurity radius as a function of the binding energy for acceptors in Ge.

tion of the correct impurity potential and the accurate form of the $\epsilon(q)$ encounters considerable difficulties. Finally, for heteropolar semiconductors, it was concluded that one has to go beyond the EMT in order to properly account for the differences in the two possible substitutional sites.

ACKNOWLEDGMENTS

One of us (J.B.) would like to thank the IBM T. J. Watson Research Center for its hospitality when this work was carried out. He would also like to thank J. C. Phillips, J. A. Appelbaum, and D. R. Hamann for stimulating discussions.

---

*Work supported in part by the Air Force Office of Scientific Research (AFSC), United States Air Force, under contract No. F49620-77-C-0005.

†Permanent address: Department of Theoretical Physics, University of Lund, Solvegatan 14A, S-223 62 Lund, Sweden.

[1]W. Kohn, in *Solid State Physics*, edited by F. Seitz and D. Turnbull (Academic, New York, 1957), Vol. 5.

[2]J. M. Luttinger and W. Kohn, Phys. Rev. 97, 869 (1955).

[3]S. T. Pantelides and C. T. Sah, Solid State Commun. 11, 1713 (1972); Phys. Rev. B 10, 621 (1974).

[4]S. T. Pantelides and C. T. Sah, Phys. Rev. B 10, 638 (1974).

[5]S. T. Pantelides, in *Festkörperprobleme*, edited by H. J. Queisser (Pergamon/Vieweg, Braunschweig, 1975), Vol. XV, p. 149.

[6]A. Baldereschi and N. O. Lipari, Phys. Rev. B 8, 2697 (1973).

[7]A. Baldereschi and N. O. Lipari, Phys. Rev. B 9, 1525 (1974).

[8]E. O. Kane, J. Phys. Chem. Solids 1, 82 (1956).

[9]J. C. Hensel, as quoted by P. Lawaetz, Phys. Rev. B 4, 3460 (1971).

[10]J. C. Hensel and K. Suzuki, Phys. Rev. Lett. 22, 838 (1969).

[11]P. Lawaetz, Ref. 9.

[12]K. Suzuki, M. Okazaki, and H. Hasegawa, J. Phys. Soc. Jpn. 19, 930 (1964).

[13]More recently, Baldereschi and Lipari (see Ref. 7) carried out calculations of acceptor binding energies in Si and Ge using the point-charge model, the full 6×6 effective-mass matrix and more flexible trial functions. See the Proceedings of the 13th International Conference on the Physics of Semiconductors, Rome, 1976 (unpublished).

[14]D. Schechter, J. Phys. Chem. Solids 23, 237 (1962).

[15]K. S. Mendelson and H. M. James, J. Phys. Chem. Solids 25, 739 (1964).

[16]K. S. Mendelson and D. R. Schultz, Phys. Status Solidi 31, 59 (1969).

[17]J. P. Walter and M. L. Cohen, Phys. Rev. B 5, 3101 (1972).

[18]H. Nara, J. Phys. Soc. Jpn. 20, 778 (1965); H. Nara and A. Morita, *ibid.* 21, 1852 (1966).

[19]R. K. W. Vinsome and D. Richardson, J. Phys. C 4, 2650 (1971).

[20]J. A. Van Vechten, Phys. Rev. 182, 891 (1969).

[21]A. Onton, P. Fischer, and A. K. Ramdas, Phys. Rev. 163, 686 (1967).

[22]R. L. Jones and P. Fischer, J. Phys. Chem. Solids 26, 1125 (1965).

[23]Quoted by A. G. Milnes, in *Deep Impurities in Semiconductors* (Wiley, New York, 1973).

[24]J. M. Herman III and C. T. Sah, Solid-State Electron. 16, 1133 (1973).

[25]I. I. Burdiyan, S. B. Mal'tsev, I. F. Mironov, and Y. G. Schreter, Fiz. Tekh. Poluprovodn. 5, 1996 (1971) [Sov. Phys.-Semicond. 5, 1734 (1972)].

[26]R. Kaplan, qupted in Ref. 6.

[27]P. J. Dean, R. A. Faulkner, S. Kimura, and M. Ilegems, Phys. Rev. B 4, 1926 (1971).

[28]P. J. Dean, C. J. Frosch, and C. H. Henry, J. Appl. Phys. 39, 5631 (1968).

[29]J. C. Phillips, *Bonds and Bands in Semiconductors* (Academic, New York, 1973), p. 238. Phillips's discussion is in terms of electronegativities of atoms.

[30]Quoted in Table 9.2 of Ref. 29.

[31]S. T. Pantelides, in *Proceedings of the Twelfth International Conference on the Physics of Semiconductors*, edited by M. H. Pilkuhn (Teubner, Stuttgart, 1973), p. 396.

[32]M. Appapillai and V. Heine, T. R. No. 5, Solid State Theory Group, Cavendish Laboratory (1972) (unpublished).